EFFECTS OF VISCOELASTICITY AND COMPRESSIBILITY ON TURBULENCE STRUCTURE FORMATION

Kiyosi Horiuti, Syouji Abe, Takao Itami, and Youhei Takagi
Department of Mechano-Aerospace Engineering,
Tokyo Institute of Technology
2-12-1 O-okayama, Tokyo 152-8552, Japan
khoriuti@mes.titech.ac.jp

ABSTRACT

A process for formation of a vortex tube along a vortex sheet and its impact on turbulence generation is investigated in the homogeneous isotropic turbulence. It is shown that a vortex tube is generated along a flat sheet under compression of the vorticity in the stretching direction. In place of the compression and reduction of the vorticity in the stretching direction, the growth of the azimuthal vorticity takes place, and the azimuthal vorticity gradually accumulates to form the vortex tube. Then, the flat sheet folds around this concentrated vortex tube, forming the spiral vortex sheet emanating from the tube core. An intense generation of turbulence takes place along the flat sheet during this sheet-tube transformation process. The effect of viscoelasticity on this sheet-tube transformation process is studied using the approximate solution for the Oldroyd constitutive equation. It is shown that the transformation process is disrupted by pulling the flat sheet back to the original flat shape, and subsequently turbulence generation is attenuated. Similar attenuation of occurrence of transformation process was found when the compressibility was introduced into the flow, but this attenuation was primarily attributed to the influence of the pressure-dilatation term.

INTRODUCTION

Coherent structures may be divided roughly into two groups: the vortex tubelike structure and the vortex sheetlike structure. Although these two structures are not distinctively separable because a vortex tube is often formed along a vortex layer during the rolling up of the layer, we consider that tube and sheet structures would primarily constitute the fundamental elements of coherent structures in turbulent flows.

In previous studies, several measures were considered for the classification of these turbulent structures, e.g., the eigenvalues, σ_1, σ_2 and σ_3, of the strain-rate tensor, $S_{ij} = (\partial u_i/\partial x_j + \partial u_j/\partial x_i)/2$. These eigenvalues are conventionally ordered such that $\sigma_1 \geq \sigma_2 \geq \sigma_3$. The eigenvectors corresponding to eigenvalues, σ_i, are denoted as $\mathbf{e}_i$ $(i = 1, 2, 3)$. In the present study, the eigenvalues σ_i $(i = 1, 2, 3)$ were reordered so that the eigenvalue, the eigenvector of which is maximally aligned with the vorticity vector, ω, is chosen as σ_z, the largest remaining eigenvalue, as σ_+, and the smallest one, as σ_-. The corresponding eigenvectors for eigenvalues, $\sigma_z, \sigma_+, \sigma_-$, were denoted as $\mathbf{e}_z, \mathbf{e}_+, \mathbf{e}_-$, respectively. This reordering was carried out to eliminate the crossover of the eigenvalues (Andreotti 1997; Horiuti 2001).

The vortex tube structures are commonly identified as the region with a positive second-order invariant of the velocity gradient tensor (Hunt *et al.* 1988)

$$Q = -\frac{1}{2}(S_{ik}S_{ki} + \Omega_{ik}\Omega_{ki}), \tag{1}$$

where Ω_{ij} is the vorticity tensor, $(\partial u_i/\partial x_j - \partial u_j/\partial x_i)/2$. Jeong & Hussain (1995) proposed a new identification method for the vortex tube, in which the eigenvalues of the symmetric tensor, $S_{ik}S_{kj} + \Omega_{ik}\Omega_{kj}$, were utilized, where the eigenvalues were denoted as λ_i $(i = 1, 2, 3)$, ordered such that $\lambda_1 \geq \lambda_2 \geq \lambda_3$. The vortex core was defined as the region with $\lambda_2 < 0$.

The entire turbulent field can be decomposed based on the magnitudes of the strain rate and the vorticity. The structure of a region in which strain rate is dominant is similar to that of a cylindrical sheet around the core of a Burgers' vortex tube model (Batchelor 1967) (curved sheet), and a vorticity-dominated region is similar to a core region of a Burgers' vortex tube model (tube core), and the region in which the magnitudes of vorticity and strain rate are comparable and large is similar to a Burgers' vortex layer model (flat sheet). It was shown in Horiuti (2001) that the curved sheet can be effectively identified by imposing the condition on the two reordered eigenvalues, $\lambda_\pm$, as $\lambda_+ \geq \lambda_- > 0$, while the flat sheet can be identified as $\lambda_+ \geq 0 \geq \lambda_-$, and the tube core as $0 > \lambda_+ \geq \lambda_-$. Although the flat sheet can be identified using the isosurfaces of the λ_- eigenvalue with negative values, when this eigenvalue was used, the tube core as well as the flat sheet were identified. In Horiuti (2003a), it was shown that the magnitude of the eigenvalue for the tensor, $-(S_{ik}\Omega_{kj} + S_{jk}\Omega_{ki})$, $[-(S_{ik}\Omega_{kj} + S_{jk}\Omega_{ki})]_+$ is very large in the vicinity of the centre of the vortex sheet similar to Burgers' vortex layer model, i.e., the flat sheet. Thus, for identifying the flat sheet by isolating it from the tube core, the isosurfaces for the eigenvalue, $[-(S_{ik}\Omega_{kj} + S_{jk}\Omega_{ki})]_+$, performs better than those of λ_-.

This identification method for the flat sheet region was used in Horiuti (2003 b) to reveal the mechanism of a process for formation of a vortex tube along a flat sheet. Direct numerical simulation (DNS) data for incompressible homogeneous isotropic turbulence was utilized. Consistency of the process obtained using the visualization of the time evolution of the structures with the development in time of the variables representing the structures estimated using the analytical solutions for these variables was presented. In addition, it was shown that intense generation of turbulence takes place associated with this sheet-tube transformation process. It is well known that the turbulence generation is markedly suppressed in the polymer diluted fluid due to its viscoelastic effect (Oldroyd 1950). It is also known that the generation of vorticity is significantly reduced when the compressible effect is introduced into the flow. We speculate

that by annihilating the occurrence of this transformation process, the generation of turbulence may be reduced. The purpose of this study is to investigate the effect of viscoelasticity and compressibility on the sheet-tube transformation process.

A SHEET-TUBE TRANSFORMATION PROCESS

A process derived using DNS data

We have utilized the DNS data for incompressible decaying homogeneous isotropic turbulence, which were generated with 256, 256 and 256 grid points, respectively, in the x, y and z directions. Periodic boundary conditions were imposed in the three directions. The size of the computational domain was 2π in each direction, the viscosity $\nu = 0.00014$, and the time interval, Δt, was set equal to 0.0005. For details of the DNS data, see Horiuti (2001). Assessment was done using the data at the instant when the Reynolds number based on the Taylor microscale, $R_\lambda \approx 88$.

Figure 1 shows the isosurfaces for the second-order invariant, Q, and the eigenvalue of the $-(S_{ik}\Omega_{kj} + S_{jk}\Omega_{ki})$ term, $[-(S_{ik}\Omega_{kj} + S_{jk}\Omega_{ki})]_+$, obtained from DNS at $t = 1.75$. It can be seen in fig. 1 that, the flat sheet structure, which were identified using the eigenvalue, $[-(S_{ik}\Omega_{kj} + S_{jk}\Omega_{ki})]_+$, and drawn using the white meshes, is formed. As can be seen in 2, which shows the isosurfaces at a later stage ($t = 1.8$), the isosurface of Q, which were drawn in the black color, concentrates at certain location along the flat sheet. At this location, compression of the vorticity in the stretching ($z-$)direction takes place.

The time evolution of this flat sheet during the duration of time between $t = 1.850$ and $t = 1.925$ is shown in the Newtonian case of fig. 6 (see the bottom page). The azimuthal vorticity gradually accumulate to form the vortex tube along the flat sheet. Then, the flat sheet folds around this concentrated vortex tube, forming the spiral vortex sheet emanating from the tube core. This sheet-tube transformation process is different from the focusing of vorticity considered by Neu (1984), in which the assumed direction of vorticity for the tube was always the $z-$direction, and the vortex tube structure shown in fig. 6 is different from that of a Burgers' vortex tube model. It should be noted that an energy cascade took place during this transformation process, and an intense generation of turbulence occurred along the flat sheet (Horiuti 2001).

Consistency with analytical eigenvalue solutions

To examine the consistency of the sheet-tube transformation process which was obtained using the DNS data with the analytical estimate of the time evolution of the variables which represent this process, we derived the governing equations for the strain-rate eigenvalues, and the vorticities.

The governing equations for the eigenvalues, σ_z, σ_+, on the basis of the principal strain eigenvectors, $\mathbf{e}_+, \mathbf{e}_-, \mathbf{e}_z$, can be derived as follows (Nomura & Post 1998).

$$\frac{D}{Dt}\sigma_z = -\sigma_z^2 + \frac{1}{4}\left(\omega_+^2 + \omega_-^2\right) - \widetilde{\Pi}_{zz}, \qquad (2)$$

$$\frac{D}{Dt}\sigma_+ = -\sigma_+^2 + \frac{1}{4}\left(\omega_-^2 + \omega_z^2\right) - \widetilde{\Pi}_{++}, \qquad (3)$$

where Π_{ij} is the pressure Hessian ($= \partial^2 p/\partial x_i/\partial x_j$), and $\widetilde{\Pi}_{ij}$ is the pressure Hessian on the basis of the principal strain eigenvectors, $\mathsf{E}^\mathsf{T}(\Pi_{ij})\mathsf{E}$. The matrices, E and E^T, are orthogonal matrices whose rows and columns, respectively, are $\mathbf{e}_+, \mathbf{e}_-, \mathbf{e}_z$. $\omega_+, \omega_-, \omega_z$ are the vorticity components projected onto the basis of the principal strain eigenvectors, $\omega \cdot \mathbf{e}_+, \omega \cdot \mathbf{e}_-, \omega \cdot \mathbf{e}_z$, respectively.

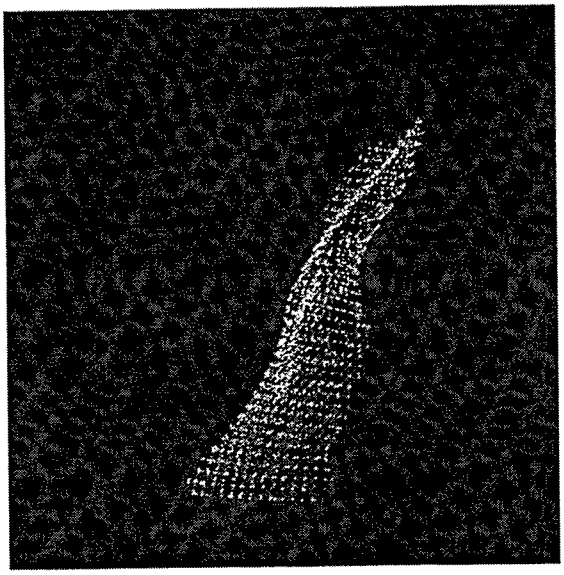

Figure 1: Isosurfaces of the $[-(S_{ik}\Omega_{kj} + S_{jk}\Omega_{ki})]_+$ eigenvalue (drawn using the white meshes), and Q (drawn using the black color), obtained from DNS at $t = 1.75$.

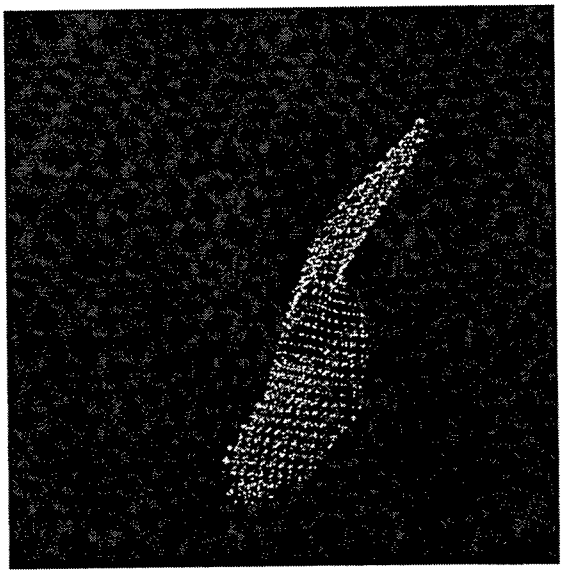

Figure 2: Isosurfaces of the sheet (white mesh) and tube (black), obtained from DNS at $t = 1.8$.

On the flat sheet, the initial strain state is $\sigma_z > 0$, $\sigma_z > \sigma_+$, and the vorticity state is $\omega_z^2 \gg \omega_+^2 > \omega_-^2$. Thus, $\frac{D}{Dt}\sigma_z < 0$ due to a large negative value of $-\sigma_z^2$, the strain state, $\sigma_z > 0$, tends to be transformed into the state, $\sigma_z < 0$, with lapse of time. Via the continuity equation, the strain state becomes $\sigma_+ > 0 > \sigma_z$. This growth of the eigenvalue, σ_+, can be also derived using Eq. (3) since the magnitude of the ω_z^2 term in the right hand side of Eq. (3) is large.

The governing equation for the vorticities, ω_z, ω_+, on the same basis can be derived as follows.

$$\frac{D}{Dt}\left(\frac{1}{4}\omega_z^2\right) = \sigma_z\omega_z^2 - \frac{1}{4}\frac{\omega_z\omega_+}{\sigma_z - \sigma_+}\widetilde{\Pi}_{z+}, \qquad (4)$$

$$\frac{D}{Dt}\left(\frac{1}{4}\omega_+^2\right) = \sigma_+\omega_+^2 - \frac{1}{4}\frac{\omega_z\omega_+}{\sigma_+ - \sigma_z}\widetilde{\Pi}_{+z}. \qquad (5)$$

Due to occurrence of compression in the $z-$direction ($\sigma_z < 0$), the magnitude of ω_z^2 decreases, while that of the azimuthal vorticity, ω_+^2, increases in turn since $\sigma_+ > 0$.

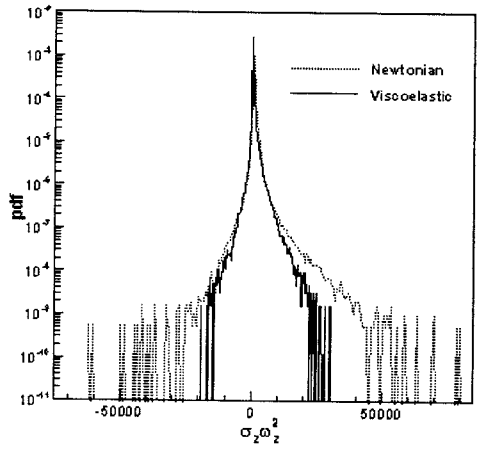

Figure 3: PDF for the $\sigma_z\omega_z^2$ term. Newtonian is from the Newtonian case, and Viscoelastic is from the viscoelastic case.

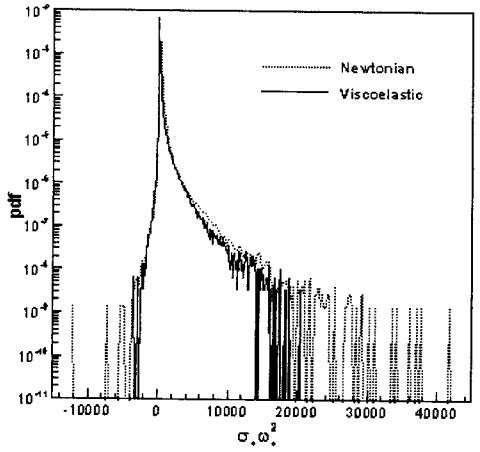

Figure 4: PDF for the $\sigma_+\omega_+^2$ term. Newtonian is from the Newtonian case, and Viscoelastic is from the viscoelastic case.

Figures 3 and 4, respectively, show the probability density functions (PDF) for the $z-$component of the vortex-stretching term, $\sigma_z\omega_z^2$, and that for the vortex-stretching term in the azimuthal direction, $\sigma_+\omega_+^2$, obtained using the DNS data. The occurrence of the compression in the stretching ($z-$)direction is in fact discernible as large negative values in the Newtonian case shown in fig. 3. In place of the compression and reduction of ω_z^2, the azimuthal component of the vortex-stretching term, $\sigma_+\omega_+^2$, takes predominantly positive value as can be seen in the Newtonian case shown in fig. 4. Thus, the azimuthal vorticity, ω_+^2, grows in time.

When the compression takes place in the stretching direction, the pressure field reacts to relax this compression. An estimate of the pressure Hessian term obtained using the DNS data showed that the $\omega_z\omega_+\widetilde{\Pi}_{z+}$ term in Eqs. (4) and (5) was predominantly negative, thus, predominantly,

$$\frac{\omega_z\omega_+}{\sigma_z - \sigma_+}\widetilde{\Pi}_{z+} > 0. \qquad (6)$$

Thus, the pressure Hessian terms in Eq. (4) and Eq. (5) react to decrease the magnitude of ω_z^2 and increase that of ω_+^2, respectively. The $\widetilde{\Pi}_{z+}$ term tends to relax the occurrence of compression in the stretching direction by forming the concentrated low pressure region oriented in the azimuthal direction, that is, the core region of the vortex tube with the azimuthal vorticity is formed.

The eigenvalue of the $-(S_{ik}\Omega_{kj} + S_{jk}\Omega_{ki})$ term, $[-(S_{ik}\Omega_{kj} + S_{jk}\Omega_{ki})]_+$ is approximately equal to $(\sigma_+ - \sigma_-)\omega_z$. The governing equation for the $(\sigma_+ - \sigma_-)\omega_z$ term can be derived as

$$\frac{D}{Dt}\left[(\sigma_+ - \sigma_-)\omega_z\right] = 2\sigma_z\left[(\sigma_+ - \sigma_-)\omega_z\right] \qquad (7)$$
$$-\frac{1}{4}\left(\frac{\omega_+^2}{\sigma_z - \sigma_+} + \frac{\omega_-^2}{\sigma_z - \sigma_-}\right)\left[(\sigma_+ - \sigma_-)\omega_z\right]$$
$$-\left(\widetilde{\Pi}_{++} - \widetilde{\Pi}_{--}\right)\omega_z - \frac{1}{4}\left(\omega_+^2 - \omega_-^2\right)$$
$$-\frac{1}{4}\frac{\sigma_+ - \sigma_-}{\sigma_z - \sigma_+}\omega_+\widetilde{\Pi}_{z+} - \frac{1}{4}\frac{\sigma_+ - \sigma_-}{\sigma_z - \sigma_-}\omega_-\widetilde{\Pi}_{z-}.$$

Because the predominant term in the right hand side of Eq. (7) was the $2\sigma_z\left[(\sigma_+ - \sigma_-)\omega_z\right]$ term, when $\sigma_z < 0$ the magnitude of the $(\sigma_+ - \sigma_-)\omega_z$ term decreased with lapse of time, i.e., with the occurrence of compression, the source term for generation of the flat sheet region diminishes.

In a Burgers' vortex layer model, using the analytical solution of the pressure Hessian term contained in Eq. (7), $(\widetilde{\Pi}_{++} - \widetilde{\Pi}_{--})$, Eq. (7) can be rearranged approximately as

$$\frac{D}{Dt}\left[(\sigma_+ - \sigma_-)\omega_z\right] = \qquad (8)$$
$$\left(2 + \frac{8S_{12}^2}{(\sigma_+^2 + S_{12}^2)(\sigma_-^2 + S_{12}^2)}\right)\sigma_z\left[(\sigma_+ - \sigma_-)\omega_z\right]$$
$$-\frac{1}{4}\left(\frac{\omega_+^2}{\sigma_z - \sigma_+} + \frac{\omega_-^2}{\sigma_z - \sigma_-}\right)\left[(\sigma_+ - \sigma_-)\omega_z\right]$$

Since the prefactor coefficient for the second term in the right hand side of Eq. (8) is positive, and the coefficient of the third term is positive, the magnitude of the $[(\sigma_+ - \sigma_-)\omega_z]$ term is reduced, when compression occurs along a Burgers' vortex layer. It can be also seen in Eq. (8) that the governing equation for the $[(\sigma_+ - \sigma_-)\omega_z]$ term is nearly autonomous, implying that if the $[(\sigma_+ - \sigma_-)\omega_z]$ term is equal to zero at the initial state, this term may never be produced in a later time evolution. The mechanism for the generation of the flat sheet region is not yet revealed. Its generation may occur through the initial setup of the flow or via the amalgamation of the random background fluctuations in a turbulent flow. Its detailed analysis will be left to future works. We note that the $(\widetilde{\Pi}_{++} - \widetilde{\Pi}_{--})$ term vanishes in a Burgers' vortex tube model, thus the pressure Hessian term makes no significant contribution to the development of the $[(\sigma_+ - \sigma_-)\omega_z]$ term in the (axially-symmetric) tube core region.

In summary, it is shown that analytical estimate of the time evolution of the representative variables is overall consistent with a scenario of the transformation process derived using the DNS data. For details, see Horiuti (2003b).

VISCOELASTIC EFFECT ON THE SHEET-TUBE TRANSFORMATION PROCESS

We consider that it may be possible to attenuate the turbulence generation by terminating the occurrence of the sheet-tube transformation observed in the previous section,. One of the well-known phenomenon for turbulence reduction is the drag reduction by dilute polymer additives (e.g., Sureshkumar, Beris & Handel 1997). In this section, we investigate the effect of viscoelasticity on the sheet-tube transformation process using the Oldroyd constitutive equation which provides a fair representation of a viscoelastic fluid (Oldroyd 1950).

The constitutive equation for the Oldroyd-A fluid can be given with the Navier–Stokes equations as

$$\frac{\partial u_i}{\partial t}+\frac{\partial (u_i u_j)}{\partial x_j}=-\frac{\partial p}{\partial x_i}+\beta\nu\frac{\partial^2 u_i}{\partial x_k \partial x_k}-(1-\beta)\frac{\nu}{\lambda}\frac{\partial c_{ij}}{\partial x_j}, \quad (9)$$

$$\frac{\partial c_{ij}}{\partial t}+u_k\frac{\partial c_{ij}}{\partial x_k}=-(c_{ik}\frac{\partial u_k}{\partial x_j}+\frac{\partial u_k}{\partial x_i}c_{kj})-\frac{1}{\lambda}(c_{ij}-\delta_{ij}), \quad (10)$$

where c_{ij} denotes the conformation stress tensor, λ the relaxation time, and β the ratio of solvent viscosity contribution to total viscosity of solution. An approximate solution for the Oldroyd-A model can be derived as follows with the initial condition at $t=0$ of $c_{ij}(0)=\delta_{ij}$.

$$c_{ij}(t)\approx\delta_{ij}-\int_0^t \mathrm{e}^{-\frac{t-s}{\lambda}}2S_{ij}(s)ds \quad (11)$$

$$+\int_0^t dr\int_0^r ds\,\mathrm{e}^{-\frac{t-s}{\lambda}}2\left(S_{ik}(s)\frac{\partial u_k}{\partial x_j}(r)+\frac{\partial u_k}{\partial x_i}(r)S_{kj}(s)\right),$$

in which the convective terms were discarded. The approximate solution, Eq. (11), contains the time-memory effect, which is important to describe the behavior of the viscoelastic fluid since a material that has no memory cannot be elastic. When the steady state is assumed, Eq. (11) can be approximated as

$$c_{ij}(t)\approx\delta_{ij}-2\lambda S_{ij}+2\lambda^2\{2S_{ik}S_{kj}+(S_{ik}\Omega_{kj}+S_{jk}\Omega_{ki})\}. \quad (12)$$

The approximation for the conformation stress tensor, c_{ij}, derived using the Oldroyd-A constitutive equation is analogous to the approximation for the subgrid-scale (SGS) stress tensor obtained using the SGS nonlinear model (Clark *et al.*1979; Horiuti 2003a).

We carried out DNS in which viscoelasticity was introduced using Eqs. (9), (10) and (12). The same flow field was considered using the same parameter values as those shown in the previous section, and $\lambda=0.36$ and $\beta=0.8$. The initial values used for this computation were the DNS data at $t=1.75$ shown in fig. 1. Using the rms value of the $S_{ik}S_{ki}$ term to estimate a characteristic strain rate, κ, of the flow, the estimate for the Weissenberg number, We, was yielded as $We=\lambda\kappa\approx 7.8$ at $t=1.75$.

In fig. 6, we included the time evolution of the isosurfaces of the eigenvalue, $[-(S_{ik}\Omega_{kj}+S_{jk}\Omega_{ki})]_+$, and Q during the duration of time between $t=1.850$ and $t=1.925$ obtained for the viscoelastic case (denoted as viscoelastic). It can be seen in fig. 6 that, the flat sheet structures are formed in both the Newtonian and viscoelastic cases, but the generation of the flat sheets is more abundant in the viscoelastic case than in the Newtonian case. Accumulation of the azimuthal vorticity in the tubes generated in the viscoelastic case, however, is rather weak, and the tubes formed in the viscoelastic case appear to be more slender and shorter in length than those in the Newtonian case. The formation of the flat sheet occurs more frequently in the viscoelastic case than in the Newtonian case, but its transformation into the tube is markedly suppressed in the viscoelastic case.

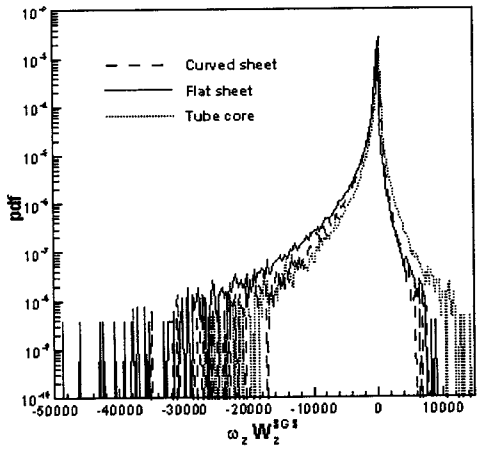

Figure 5: Distributions of PDFs for the $z-$component of the elastic enstrophy generation term, $\omega_z W_z$, due to the $(S_{ik}\Omega_{kj}+S_{jk}\Omega_{ki})$ term obtained from the viscoelastic case.

It was found that these differences were attributed to the differences in the profiles of the vortex-stretching term as well as the elastic enstrophy generation term,

$$P_\omega=\varepsilon_{ilm}\omega_i\frac{\partial^2 c_{mj}}{\partial x_l \partial x_j}, \quad (13)$$

in the Newtonian and viscoelastic cases.

In figs 3 and 4, we included the profiles of the PDFs for the vortex-stretching terms, $\sigma_z\omega_z^2$ and $\sigma_+\omega_+^2$, obtained from the viscoelastic case. It can be seen that the amplitude of the vortex-stretching terms obtained from the viscoelastic case are markedly smaller than that obtained from the Newtonian case, indicating that the sheet-tube transformation takes place less frequently in the viscoelastic case.

The elastic enstrophy generation term, P_ω, can be written as the inner product of the vorticity vector, ω, with the elastic vortex-stretching vector, $\boldsymbol{W}$, the $i-$th component of which is $W_i(=\varepsilon_{ilm}(\partial^2 c_{mj}/\partial x_l/\partial x_j))$. When ω and $\boldsymbol{W}$ are projected onto the basis of the strain-rate eigenvectors, $\mathbf{e}_+,\mathbf{e}_-,\mathbf{e}_z$, P_ω can be decomposed as

$$P_\omega=\omega_z W_z+\omega_+ W_+ +\omega_- W_-. \quad (14)$$

Figure 5 shows the PDFs for the $z-$component of this decomposed P_ω term, $\omega_z W_z$, due to the $(S_{ik}\Omega_{kj}+S_{jk}\Omega_{ki})$ term, in which c_{ij} was set equal to $(S_{ik}\Omega_{kj}+S_{jk}\Omega_{ki})$ in Eq. (13). Figure 5 was obtained from the viscoelastic case. The PDFs were decomposed into those in the curved sheet, flat sheet and tube core regions. It can be seen that the elastic enstrophy was backwardly transferred into the fluid part in all three regions, but the most intense backward transfer occurred in the flat sheet region, indicating that the vorticity in the stretching $(z-)$direction is strengthened in the flat sheet region. As a result, the $(S_{ik}\Omega_{kj}+S_{jk}\Omega_{ki})$ term tends to disrupt the transformation of the flat sheet into the vortex tube by snapping the sheet back to the original flat shape, i.e., an intense viscoelastic effect was incurred by the $(S_{ik}\Omega_{kj}+S_{jk}\Omega_{ki})$ term primarily on the flat sheet (Horiuti 2003 a,b).

Comparison of the Oldroyd A- and B- equations

An alternative constitutive equation of the conformation stress tensor, c_{ij}, is the Oldroyd-B equation as

$$\frac{\partial c_{ij}}{\partial t} + u_k \frac{\partial c_{ij}}{\partial x_k} = (c_{ik}\frac{\partial u_j}{\partial x_k} + \frac{\partial u_i}{\partial x_k} c_{kj}) - (c_{ij} + \delta_{ij}). \quad (15)$$

The approximate solution for the Oldroyd-B equation corresponding to that of the Oldroyd-A equation is derived as

$$c_{ij} \approx -\delta_{ij} - 2\lambda S_{ij} + 2\lambda^2\{-2S_{ik}S_{kj} + (S_{ik}\Omega_{kj} + S_{jk}\Omega_{ki})\}. \quad (16)$$

The approximate solution for the c_{ij} term yielded from the Oldroyd-B constitutive equation is analogous to the solution obtained using the Oldroyd-A equation (Eq. 12), and the $(S_{ik}\Omega_{kj} + S_{jk}\Omega_{ki})$ term is contained in both Oldroyd-A and Oldroyd-B solutions. It should be noted that its coefficient is $+1$, whereas that for the SGS nonlinear model is -1. It appears that this coefficient should be set equal to -1 to model the Newtonian fluids, while it should be set equal to $+1$ for the viscoelastic fluids (Horiuti 2003a).

The production term of the total kinetic energy of the fluid, $u_i u_i/2$, due to the nonlinear part of the c_{ij} term for the Oldroyd-A equation, P^A, is given as

$$P^A = (1-\beta)\frac{\nu}{\lambda} c_{ij} S_{ji} = 4(1-\beta)\nu\lambda S_{ik}S_{kj}S_{ji}, \quad (17)$$

while that for the Oldroyd-B equation, P^B, is

$$P^B = (1-\beta)\frac{\nu}{\lambda} c_{ij} S_{ji} = -4(1-\beta)\nu\lambda S_{ik}S_{kj}S_{ji}. \quad (18)$$

The generation term of the total elastic energy, $c_{ii}/2$, due to the nonlinear part of the c_{ij} term for the Oldroyd-A equation, P_c^A, is given as

$$P_c^A = -c_{ij}S_{ji} = -4\lambda^2 S_{ik}S_{kj}S_{ji}, \quad (19)$$

and that for the Oldroyd-B equation, P_c^B, is identical to the P_c^A term as

$$P_c^B = c_{ij}S_{ji} = -4\lambda^2 S_{ik}S_{kj}S_{ji}. \quad (20)$$

We note that the derivative skewness, $S_{ik}S_{kj}S_{ij}$, is generally negative on average in the homogeneous isotropic turbulence (Batchelor 1967), and that the sign of the P^A term is opposite to that of the P_c^A term, whereas the signs for the P^B and P_c^B terms are the same. Thus, in the Oldroyd-A fluid, the kinetic energy of the fluid is converted into the elastic energy on average, whereas in the Oldroyd-B fluid, the elastic energy is backwardly transformed into the kinetic energy of the fluid on average, while the elastic energy is increased simultaneously.

It should be noted that the $(S_{ik}\Omega_{kj} + S_{jk}\Omega_{ki})$ term vanishes in the P^A, P^B, P_c^A, P_c^B terms, thus this term makes no contribution to the production of the (total) energy, but this term is retained in the elastic enstrophy generation term, P_ω (Eq. (13)). We consider that this term causes a significant impact on the evolution of the viscoelastic fluid, although the time-memory effect is equally important for the viscoelastic fluid (Horiuti 2003a).

In the present study, we have shown the results obtained using the approximate solution of the Oldroyd-A constitutive equation. We have carried out the computation using a full Oldroyd-A constitutive equation. The results were similar to those shown in figs. 3, 4, 5, and 6. In the DNS using the full Oldroyd-A and -B constitutive equations, the behaviours of the energy and enstrophy exchange in their solutions were consistent with the estimate presented above.

SUMMARY

We have studied a process for the transformation of the flat sheet into the vortex tube in a homogeneous isotropic turbulence. The result obtained using the DNS data was consistent with the analytical estimate of the evolution of the variables representing the sheet and the tube structures. It was shown that when the viscoelastic effect was introduced, its effect was primarily strong on the flat sheet region, and the sheet-tube transformation process was disrupted.

For the compressible case, using the DNS data for the compressible homogeneous isotropic turbulence, we found a reduction of generation of the vorticity. Similarly to the viscoelastic case, the flat sheets were generated in the compressible flow case as well, but their transformation into the tubes was disrupted (data not shown). This disruption occurred as a result of the characteristic difference in the types of the governing equations for the pressure field. In incompressible flow, the pressure field is governed by the elliptic equation, while in compressible flow it by the equation which develops in time. The pressure-dilatation term was primarily responsible for causing the disruption of occurrence of the sheet-tube transformation and subsequent reduction of vorticity generation in compressible flow.

This work was partially supported by Grants-in-Aid from the Ministry of Education, Culture, Sports, Science and Technology, Japan (Nos. 12650156 and 14550141). Main computations were performed using the NEC SX-5 system at the Cybermedia Centre, Osaka University.

REFERENCES

Andreotti, B., 1997, "Studying Burgers' models to investigate the physical meaning of the alignments statistically observed in turbulence", *Phys. Fluids* Vol. 9, p. 735.

Batchelor, G. K., 1967, *An Introduction to Fluid Mechanics*. Cambridge Univ. Press.

Clark, R. A., Ferziger, J. H. and Reynolds, W. C., 1979, "Evaluation of subgrid-scale models using an accurately simulated turbulent flow", *J. Fluid Mech.* Vol. 91, p. 1.

Horiuti, K., 2001, "A classification method for vortex sheet and tube structures in turbulent flows", *Phys. Fluids* Vol. 13, p. 3756.

Horiuti, K., 2003a, "Roles of nonaligned eigenvectors of strain-rate and subgrid-scale stress tensors for turbulence generation", submitted to *J. Fluid Mech.*.

Horiuti, K., 2003b, "A process for formation of vortex tube along vortex sheet", in preparation.

Hunt, J. C. R., Wray, A. A., and Moin, P., 1988, "Eddies, stream, and convergence zones in turbulent flows," *Center for Turbulence Research Report* Vol. S88, p. 193.

Jeong, J. and Hussain, F., 1995, "On the identification of a vortex", *J. Fluid Mech.* Vol. 285, p. 69.

Neu, J.C., 1984, "The dynamics of stretched vortices", *J. Fluid Mech.* Vol. 143, p. 253.

Nomura, K. K. and Post, G. K., 1998, "The structure and dynamics of vorticity and rate of strain in incompressible homogeneous turbulence", *J. Fluid Mech.* Vol. 377, p. 65.

Oldroyd, J. G., 1950, "On the formulation of rheological equations of state", *Proc. Roy. Soc. London A* Vol. 200, p. 523.

Sureshkumar, R., Beris, A. N. and Handel, R. A., 1997, "Direct numerical simulation of the turbulent channel flow of a polymer solution.", *Phys. Fluids* Vol. 9, p. 743.

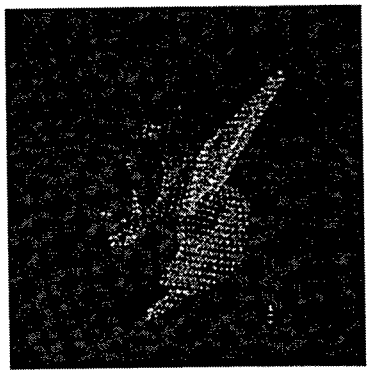

$t = 1.850$ (Newtonian)

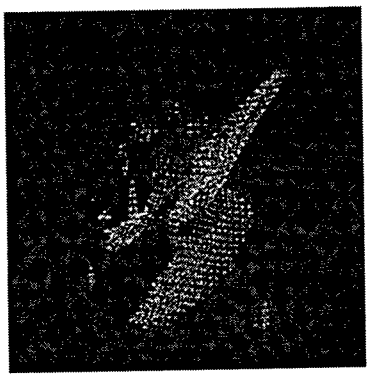

$t = 1.850$ (viscoelastic)

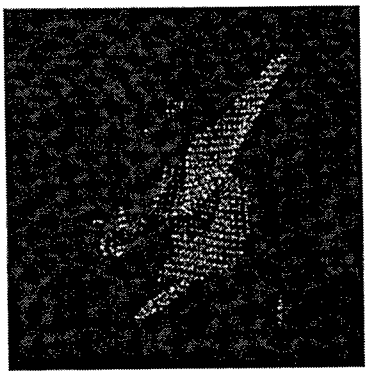

$t = 1.875$ (Newtonian)

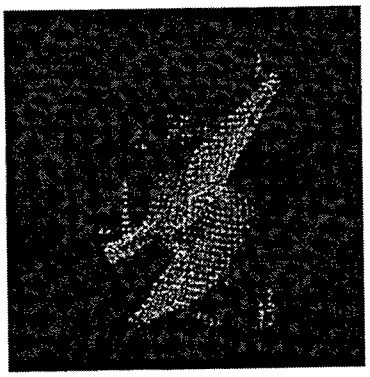

$t = 1.875$ (viscoelastic)

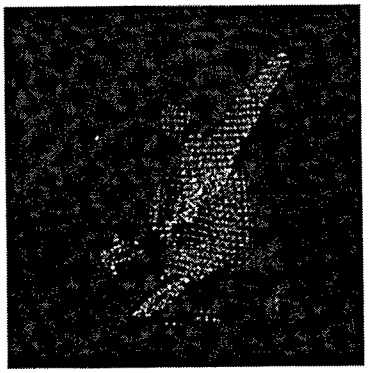

$t = 1.900$ (Newtonian)

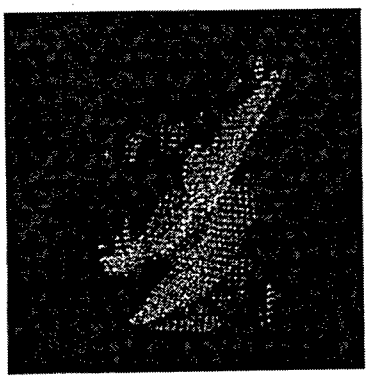

$t = 1.900$ (viscoelastic)

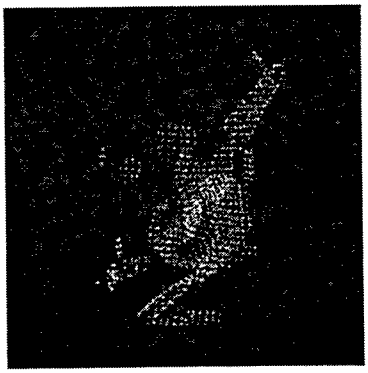

$t = 1.925$ (Newtonian)

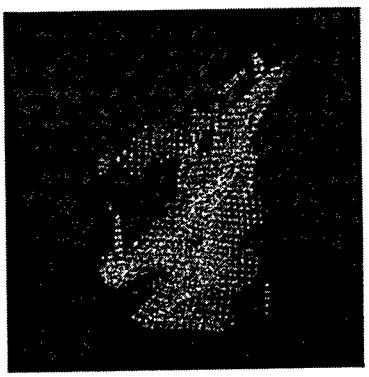

$t = 1.925$ (viscoelastic)

Figure 6: Isosurfaces of the sheet (white mesh) and the tube (black)